Astron. Astrophys. 351, 212–224 (1999)

ASTRONOMY AND ASTROPHYSICS

Time series analysis of V 1794 Cygni long–term photometry

L. Jetsu[1,2]**, J. Pelt**[3,4]**, and I. Tuominen**[4]

[1] Observatory, P.O. Box 14, University of Helsinki, 00014, Finland
[2] NORDITA, Blegdamsvej 17, 2100 Copenhagen, Denmark
[3] Tartu Observatory, 61 602 Tõravere, Estonia
[4] Astronomy Division, University of Oulu, P.O. Box 3000, 90410 Oulu, Finland

Received 8 June 1998 / Accepted 6 August 1999

Abstract. Standard Johnson UBVRI photometry of V 1794 Cyg (HD199178) between 1975 and 1995 is analysed. Instead of the traditional constant period ephemeris, we determine the seasonal periodicities ($P_{\rm phot}$) and the primary and secondary minima epochs ($t_{\rm min,1}$, $t_{\rm min,2}$) of the normalized UBVRI magnitudes using the three stage period analysis (TSPA) and complementary methods. Our $t_{\rm min,1}$ and $t_{\rm min,2}$ estimates with variable $P_{\rm phot}$ can adapt easily to both differential rotation and longitudinal activity migration. The seasonal $P_{\rm phot}$ are utilized in modelling the mean (M) and total amplitude (A) of contemporary light curves in UBVRI. TSPA reveals that the long–term M and A changes of V 1794 Cyg are *unpredictable*. We search for *active longitudes* from the $t_{\rm min,1}$ and $t_{\rm min,2}$ series of time points with nonparametric methods. The critical level of 0.0029 for the best $3.^{\rm d}3175$ period detected with the Kuiper method is high, but exceeds the 0.001 significance for rejecting the hypothesis that the phases of $t_{\rm min,1}$ and $t_{\rm min,2}$ are randomly distributed. The activity centres in V 1794 Cyg are rarely disrupted, and most probably undergo *continuous* longitudinal migration, because only one abrupt disruption is observed during 20 years. As for *differential rotation*, the irregular changes of seasonal $P_{\rm phot}$ are 7.5%. The surprisingly regular 3.3% changes of yearly $P_{\rm phot}$ may provide a stellar analogy of the solar "butterfly" diagram.

Key words: stars: individual: V 1794 Cyg – stars: variables: general – stars: activity – techniques: photometric

1. Introduction

The most distinctive aspects of sunspots, like the sunspot cycle, the latitudinal migration of activity (i.e. the "butterfly" diagram), the solar differential rotation, and the unpredictable prolonged activity suppressions, were already discovered by Schwabe (1843), Carrington (1858) and Maunder (1890, 1894). Yet, the correlation between solar magnetic activity and luminosity could be verified only recently (e.g. Willson & Hudson 1991). That starspots, being the counterparts of sunspots, induce detectable rotational and long–term luminosity variations in some late–type stars was confirmed earlier (e.g. Kron 1947; Hall 1972). The FK Comae stars are one of the 11 groups of stars, where magnetic activity has been observed (Hall 1991). Bopp & Rucinski (1981) defined this group, possibly representing coalesced W Uma binaries, as single and rapidly rotating G–K giants with strong chromospheric and transition region UV emission. The rapidly rotating giant V 1794 Cyg fulfills all FK Comae–type classification criteria: G5III-IV, $v_{\rm rad} = -27.9 \pm 1.6$ km s^{-1}(i.e. single), $P_{\rm phot} = 3.^{\rm d}337484$, and $v \sin i = 65.4$ km s^{-1}(Herbig 1958; Huenemoerder 1986; Jetsu et al. 1990a; Fekel 1997). The detections of chromospheric, transition region, and coronal activity include emission at radio (Drake et al. 1990; Walter et al. 1990), IR (Dempsey et al. 1993), CaII H, Hα (Huenemoerder 1986), UV (Bopp & Stencel 1981; Simon & Fekel 1987), and X–ray (Schachter et al. 1996) wavelengths. The common denominator between V 1794 Cyg and the Sun is magnetic activity. But in terms of the solar–stellar–connection, the rapidly rotating giant V 1794 Cyg is several factors more active than the Sun, as predicted by numerous rotation–activity–relations (e.g. Simon & Fekel 1987; Hartmann & Noyes 1987; Pasquini et al. 1990; Strassmeier et al. 1990; Böhm–Vitense 1992). We perform a detailed time series analysis of the starspot induced luminosity variations in V 1794 Cyg, and magnetic activity connected phenomena, such as flares, activity cycle(s), differential rotation and active longitudes.

2. Light curve modelling

We model the V 1794 Cyg data between 1975 and 1995: 114 subsets (SET) of UBVRI photometry with an external accuracy of $\sim 0.^{\rm m}015$ in BVRI and $\sim 0.^{\rm m}030$ in U (Jetsu et al. 1999: Paper II). The parameters of our second order ($K = 2$) light curve model

$$g(\bar{\beta}) = g(t, \bar{\beta}) = M + \sum_{\rm k=1}^{\rm K} B_{\rm k} \cos(k2\pi f t) + C_{\rm k} \sin(k2\pi f t) \quad (1)$$

are: the mean (M), the amplitudes (B_1, B_2, C_1, C_2), and the frequency (f, i.e. the period $P = f^{-1}$). The free parameter vector is $\bar{\beta} = [M, B_1, B_2, C_1, C_2, f]$ or $\bar{\beta}_{\rm f} = [M, B_1, B_2, C_1, C_2]$ for fixed f. Only subsets with nonflare observations during at least 7 nights (nts) are modelled. In Sect. 3 this model for the original

Send offprint requests to: jetsu@gstar.astro.helsinki.fi

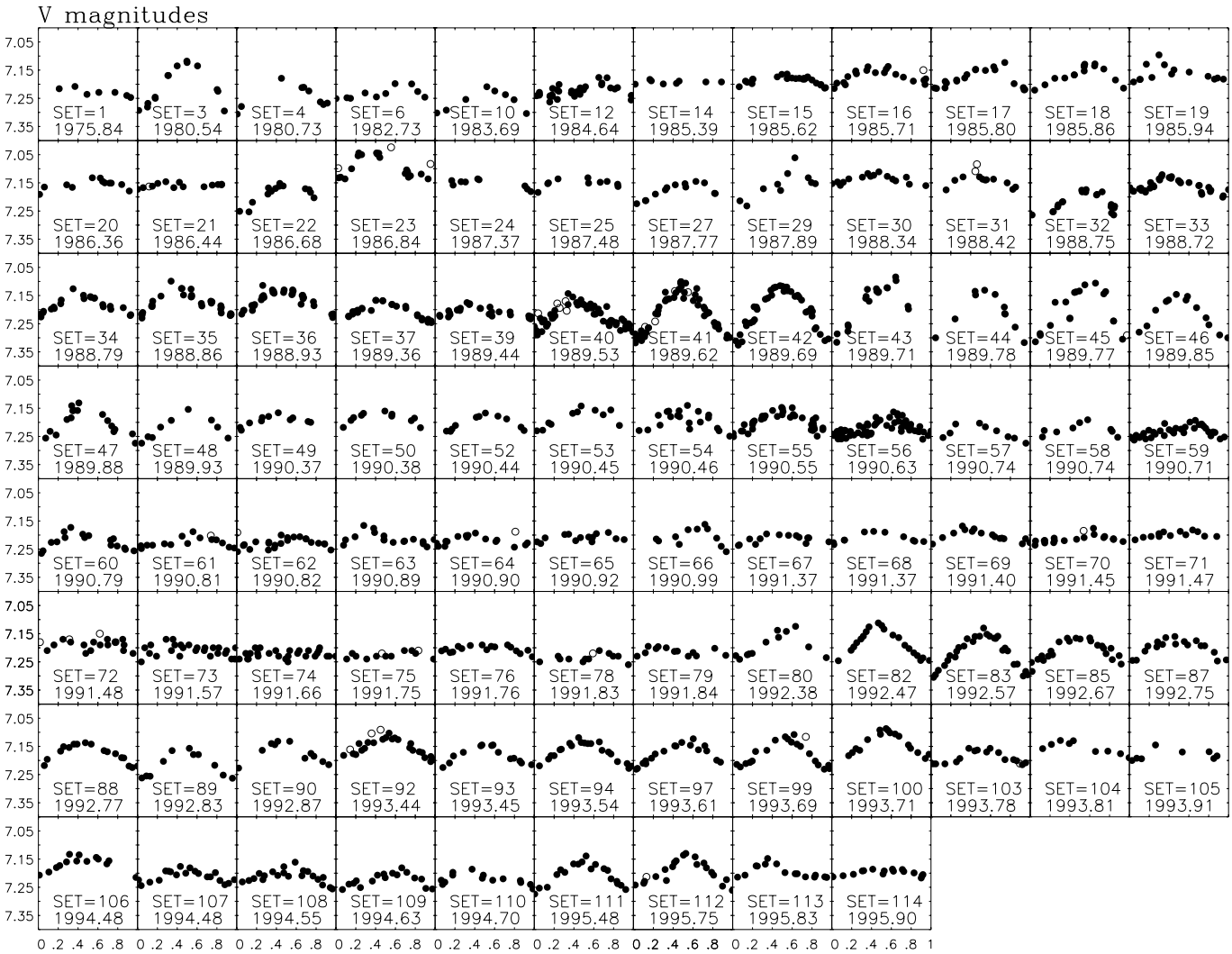

Fig. 1. The V light curves of subsets with $\mathrm{nts} \geq 7$: The ephemerides in each SET are $\mathrm{HJD}_{\min} = (t_{\min,1} + P)\mathrm{E}$ from Table 3. The nonflare and flare (F = Flare or Flare?) observations are denoted by closed and open circles, respectively

UBVRI magnitudes is *linear* with fixed f. The three stage period analysis (TSPA) by Jetsu & Pelt (1999: Paper I) with f as a free parameter is applied in Sect. 4 for the *nonlinear* modelling of the normalized magnitudes ($\bar{y}_{\mathrm{norm}}$). The nonflare data ($\bar{y}$) of every SET with $\mathrm{nts} \geq 7$ were normalized separately in each UBVRI passband with a relation based on the mean (m_{y}) and standard deviation (s_{y}) of $\bar{y}$ (Paper I: Eq. 17).

All V 1794 Cyg light curves are modelled with a varying $P = P_{\mathrm{phot}}$. The best P in each SET is determined with the TSPA applied to $\bar{y}_{\mathrm{norm}}$ from all available passbands, which also yields the primary and secondary minima *epochs* ($t_{\min,1}$, $t_{\min,2}$). The ephemerides $\mathrm{HJD}_{\min} = (t_{\min,1} + P)\mathrm{E}$ are used for the linear modelling of the mean (M) and the total amplitude (A) of the light curve in each UBVRI passband. Both M and A are nearly independent of P, because $M \approx m_{\mathrm{y}}$ and $A/s_{\mathrm{y}} \approx 2.7$ are accurate approximations for subsets with $\mathrm{nts} \geq 7$ (Paper I: Sect. 6.3). Like for any active star, the traditional constant P ephemeris for the whole data of V 1794 Cyg would overlook differential rotation and longitudinal shifts of activity centres. Our varying P approach adapts easily to these phenomena. Hence there is no unique *phase* for the *whole* data, but the phase dependent light curve features are unique in *time*, e.g. the $t_{\min,1}$ epoch does not depend strongly on P changes of a few percent (see Jetsu et al. 1993: Fig. 8). The phases are $\phi = \mathrm{FRAC}[(t - t_{\min,1})P^{-1}]$ within each SET, where FRAC removes the integer part of $(t - t_{\min,1})P^{-1}$. In conclusion, first the nonlinear TSPA modelling of $\bar{y}_{\mathrm{norm}}$ yields P, $t_{\min,1}$ and $t_{\min,2}$ of each SET, and then the linear modelling of the UBVRI magnitudes with $\mathrm{HJD}_{\min} = (t_{\min,1} + P)\mathrm{E}$ gives M_{U}, M_{B},..., M_{I}, A_{U}, A_{B},..., A_{R} and A_{I}. The M, A, $t_{\min,1}$, $t_{\min,2}$ and P errors are estimated with the bootstrap explained in Paper I (Sect. 4).

The results of this varying period analysis of V 1794 Cyg are presented in four separate tables. The mean and the total amplitude of the UBVR light curves during each SET are given in Table 1 (M and A). The analysis of a series of time points, the primary and secondary minima epochs of these lights curves, is summarized in Table 2. The results of the time series anal-

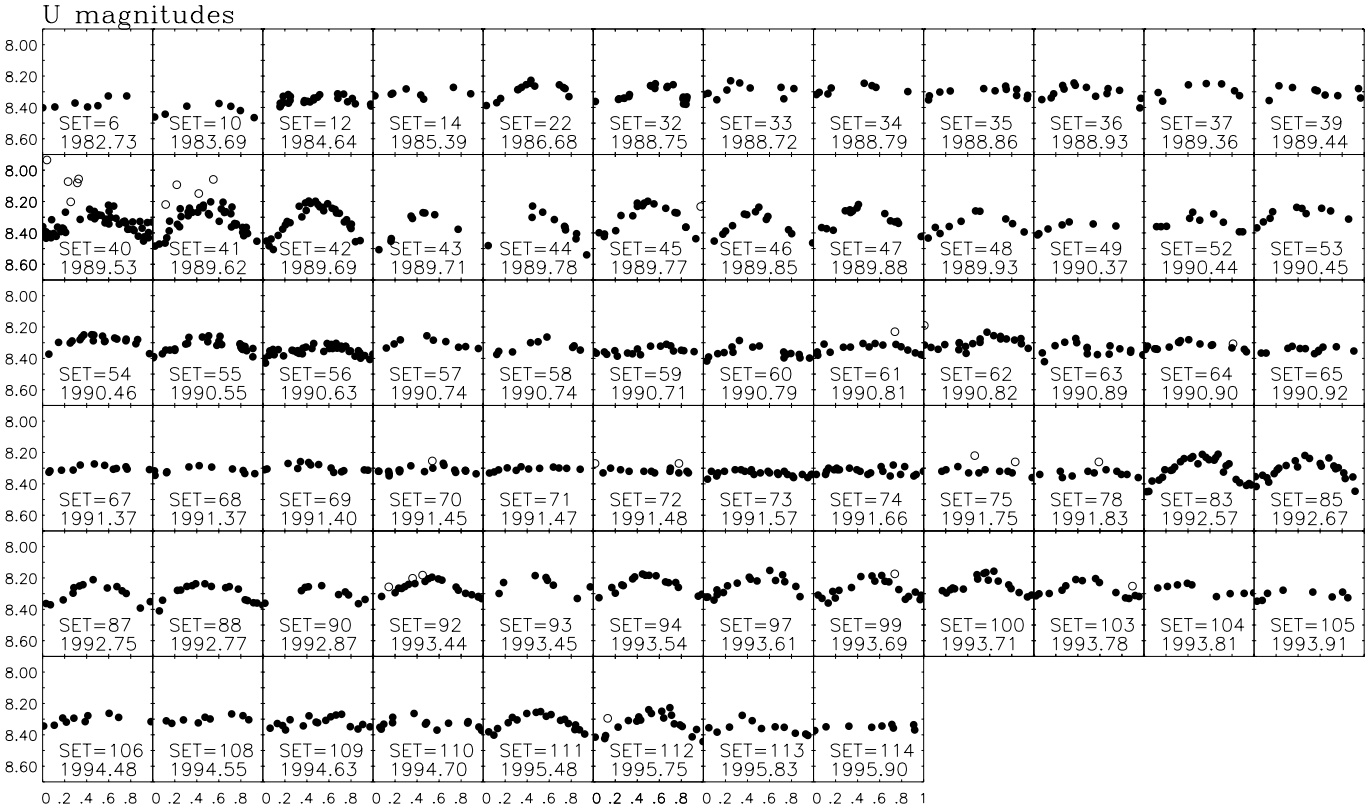

Fig. 2. The U light curves for subsets with $\mathrm{nts} \geq 7$, otherwise as in Fig. 1

ysis of the normalized magnitudes within each SET are given in Table 3 (P, $t_{\min,1}$ and $t_{\min,2}$). The last Table 4 presents the predictions for the changes in the yearly primary minima.

3. Original UBVRI magnitudes

This section studies the M and A of each SET with a linear model (Eq. 1), where $f = P^{-1}$ and $\mathrm{HJD}_{\min} = (t_{\min,1} + P)\mathrm{E}$ are from Table 3.

3.1. Flares

We found no earlier photometric flare detections for V 1794 Cyg, nor reported any in Jetsu et al. (1990a, 1990b). All UBVRI light curves were analysed with the flare detection procedure applied earlier for FK Com (Jetsu et al. 1993). It relies on the light curve residuals, and on the regular linear dependence between nonflare measurements in two arbitrary UBVRI magnitudes (Jetsu et al. 1993: Figs. 1, 2 and 3). Flares are above the light curve and violate the aforementioned linearity, especially in UB. Flares were identified in 19 subsets, including 4 in Jetsu et al. (1990a, 1990b). Our "Flare" and "Flare?" notations are as in Jetsu et al. (1993): U–band data were available only for the former ones, and thus the latter identifications are uncertain, the flares deviating less in BVRI (compare Figs. 1 and 2). These deviations were excluded before the light curve modelling and the determination of $\bar{y}_{\mathrm{norm}}$, regardless of whether they represent real flares or observational errors. If flares, these are most probably of short duration, because two successive measurements possibly representing a *single* event were recorded only during SET=40. But except for a few subsets, V 1794 Cyg was observed only once or twice each night, which prevents an indisputable flare identification, such as e.g. in Jetsu et al. (1993: Fig. 1). Apart from flares or observational errors, rapid light curve changes might induce some of these deviations (e.g. Fig. 1: SET=112), because an adequate light curve phase coverage requires a subset length of about 30^{d}. Unlike FK Com (Jetsu et al. 1993: Fig. 6b), V 1794 Cyg seems to have no preferred flaring phase with respect to the light maximum (Figs. 1 and 2). Henry & Newsom (1996) detected only five photometric flares in 17207 measurements of 69 chromospherically active evolved stars. Those flare detections for UX Ari, II Peg, and AR Psc coincided with light curve maxima, as also for FK Com (Jetsu et al. 1993). Our flare analysis for V 1794 Cyg resembles that by Henry & Newsom (1996), except that the F=Flare? events were identified without U–band data, and are therefore less reliable.

3.2. Activity cycles: the M and A changes

Fig. 3 displays the M_{B}, M_{V}, M_{B}–M_{V}, A_{B}, and A_{V} changes for subsets with $\mathrm{nts} \geq 7$. Table 1 gives all M and A in UBVR. Only four subsets had $\mathrm{nts} \geq 7$ in I. These SET=6, 10, 22 and 32 had $M_{\mathrm{I}} = 6.159 \pm 0.002, 6.179 \pm 0.002, 6.123 \pm 0.003$ and 6.144 ± 0.002 combined with $A_{\mathrm{I}} = 0.0470 \pm 0.0077$, 0.0766 ± 0.0038, 0.063 ± 0.011 and 0.0746 ± 0.0067, respectively. For example,

Table 1. The means ($M_{\rm U}$, $M_{\rm B}$, $M_{\rm V}$ and $M_{\rm R}$) and total amplitudes ($A_{\rm U}$, $A_{\rm B}$, $A_{\rm V}$ and $A_{\rm R}$) for the modelled UBVR light curves of subsets with $\mathrm{nts} \geq 7$

SET	Epoch	$M_{\rm U}$	$A_{\rm U}$	$M_{\rm B}$	$A_{\rm B}$	$M_{\rm V}$	$A_{\rm V}$	$M_{\rm R}$	$A_{\rm R}$
1	1975.84			8.0144(.0005)	0.0536(.0020)	7.229(.001)	0.0465(.0052)	6.562(.001)	0.0276(.0048)
3	1980.54			8.019(.002)	0.2129(.0057)	7.205(.002)	0.1831(.0080)		
4	1980.73			8.05(.01)	0.146(.027)	7.226(.008)	0.122(.022)		
6	1982.73	8.370(.003)	0.099(.011)	7.991(.001)	0.0798(.0058)	7.231(.002)	0.0684(.0065)	6.565(.002)	0.0518(.0068)
10	1983.69	8.4126(.0008)	0.0926(.0025)	8.019(.002)	0.1013(.0067)	7.259(.002)	0.0896(.0056)	6.5848(.0008)	0.0763(.0019)
12	1984.64	8.356(.004)	0.073(.014)	8.008(.002)	0.0712(.0070)	7.222(.002)	0.0533(.0076)		
14	1985.39	8.311(.004)	0.067(.012)	7.976(.001)	0.0281(.0046)	7.192(.002)	0.0123(.0061)		
15	1985.62			7.954(.001)	0.0389(.0076)	7.186(.001)	0.0454(.0070)		
16	1985.71			7.941(.003)	0.0656(.0077)	7.170(.003)	0.0576(.0064)		
17	1985.80			7.950(.002)	0.1160(.0067)	7.177(.002)	0.0855(.0073)		
18	1985.86			7.948(.002)	0.1126(.0057)	7.176(.002)	0.0919(.0049)		
19	1985.94			7.967(.006)	0.090(.022)	7.163(.005)	0.067(.015)		
20	1986.36			7.912(.002)	0.0731(.0076)	7.159(.003)	0.0401(.0067)		
21	1986.43			7.920(.001)	0.0497(.0050)	7.161(.002)	0.0197(.0054)		
22	1986.68	8.308(.003)	0.175(.020)	7.929(.002)	0.140(.013)	7.199(.002)	0.104(.012)	6.524(.004)	0.078(.015)
23	1986.83					7.096(.002)	0.1113(.0061)		
24	1987.37			7.878(.007)	0.197(.032)	7.129(.007)	0.125(.032)		
25	1987.48			7.909(.003)	0.081(.013)	7.149(.002)	0.057(.010)		
27	1987.77			7.962(.002)	0.0972(.0076)	7.182(.001)	0.0808(.0051)		
29	1987.89			7.943(.007)	0.199(.032)	7.170(.006)	0.159(.027)		
30	1988.34			7.925(.002)	0.0485(.0049)	7.139(.002)	0.0353(.0049)		
31	1988.42			7.935(.002)	0.0502(.0076)	7.156(.002)	0.0775(.0084)		
32	1988.75	8.323(.004)	0.124(.014)	7.947(.003)	0.105(.012)	7.226(.002)	0.0954(.0089)	6.553(.004)	0.097(.014)
33	1988.73	8.296(.009)	0.099(.032)	7.938(.002)	0.0595(.0054)	7.162(.002)	0.0527(.0049)		
34	1988.79	8.279(.004)	0.082(.015)	7.954(.002)	0.0986(.0065)	7.181(.002)	0.0791(.0054)		
35	1988.86	8.299(.006)	0.063(.014)	7.943(.003)	0.119(.010)	7.169(.002)	0.1121(.0069)		
36	1988.93	8.309(.005)	0.124(.016)	7.948(.001)	0.1020(.0031)	7.171(.002)	0.0876(.0049)		
37	1989.36	8.291(.006)	0.103(.027)	7.983(.002)	0.0909(.0045)	7.205(.001)	0.0682(.0037)		
39	1989.44	8.300(.007)	0.086(.026)	7.982(.002)	0.0544(.0047)	7.209(.001)	0.0439(.0046)		
40	1989.53	8.341(.006)	0.114(.014)	8.014(.003)	0.111(.010)	7.218(.002)	0.1011(.0068)	6.545(.002)	0.0814(.0055)
41	1989.62	8.339(.006)	0.231(.017)	8.006(.002)	0.2123(.0055)	7.210(.002)	0.1838(.0037)	6.541(.002)	0.1540(.0044)
42	1989.69	8.338(.005)	0.273(.014)	7.998(.003)	0.2208(.0092)	7.208(.002)	0.1919(.0065)	6.541(.002)	0.1645(.0071)
43	1989.71	8.379(.002)	0.2384(.0078)	7.990(.007)	0.257(.028)	7.202(.005)	0.214(.016)		
44	1989.78	8.36(.02)	0.258(.046)	8.0074(.0010)	0.2007(.0032)	7.220(.003)	0.1846(.0068)		
45	1989.77	8.312(.005)	0.232(.014)	7.989(.007)	0.258(.026)	7.206(.006)	0.237(.021)	6.540(.004)	0.174(.016)
46	1989.85	8.366(.003)	0.200(.011)	8.008(.002)	0.1722(.0063)	7.223(.002)	0.1508(.0043)		
47	1989.88	8.318(.004)	0.179(.017)	7.984(.004)	0.180(.015)	7.202(.003)	0.132(.012)	6.532(.003)	0.110(.011)
48	1989.94	8.334(.004)	0.165(.017)	7.991(.003)	0.128(.010)	7.209(.002)	0.1195(.0058)		
49	1990.37	8.364(.002)	0.0798(.0059)	7.982(.002)	0.0665(.0061)	7.197(.002)	0.0481(.0056)		
50	1990.38			7.966(.002)	0.0991(.0085)	7.189(.002)	0.0664(.0078)		
52	1990.44	8.341(.005)	0.115(.016)	7.9884(.0008)	0.0897(.0028)	7.203(.001)	0.0680(.0031)		
53	1990.45	8.281(.004)	0.147(.014)	7.963(.003)	0.098(.012)	7.185(.003)	0.0774(.0097)		
54	1990.46	8.299(.004)	0.097(.013)	7.972(.006)	0.099(.016)	7.201(.004)	0.078(.015)	6.531(.004)	0.078(.012)
55	1990.55	8.322(.003)	0.109(.010)	7.984(.002)	0.0904(.0073)	7.198(.002)	0.0777(.0061)	6.533(.002)	0.0668(.0056)
56	1990.63	8.353(.003)	0.0699(.0093)	8.018(.002)	0.0591(.0068)	7.221(.002)	0.0536(.0058)	6.557(.002)	0.0373(.0043)
57	1990.74	8.302(.002)	0.0953(.0093)	8.001(.002)	0.0848(.0093)	7.234(.001)	0.0874(.0060)		
58	1990.74	8.326(.003)	0.1004(.0090)	8.001(.003)	0.094(.020)	7.226(.002)	0.080(.012)		
59	1990.71	8.351(.003)	0.055(.011)	8.027(.002)	0.0505(.0069)	7.234(.002)	0.0497(.0058)	6.564(.002)	0.0383(.0063)
60	1990.79	8.360(.004)	0.094(.014)	8.015(.004)	0.086(.011)	7.223(.002)	0.0754(.0067)	6.566(.004)	0.056(.011)
61	1990.81	8.332(.004)	0.063(.014)	8.005(.003)	0.0436(.0075)	7.225(.002)	0.0411(.0073)		
62	1990.82	8.302(.004)	0.075(.013)	8.003(.002)	0.0524(.0060)	7.229(.002)	0.0386(.0058)		
63	1990.89	8.344(.005)	0.116(.018)	8.007(.002)	0.0582(.0080)	7.212(.002)	0.0611(.0080)	6.550(.003)	0.0429(.0093)
64	1990.90	8.321(.002)	0.0550(.0062)	7.994(.001)	0.0424(.0036)	7.221(.002)	0.0377(.0049)		
65	1990.92	8.345(.003)	0.0473(.0091)	7.994(.002)	0.0414(.0064)	7.208(.002)	0.0352(.0075)		
66	1990.99			8.000(.007)	0.116(.021)	7.217(.004)	0.105(.013)	6.551(.003)	0.106(.014)

Table 1. (continued)

SET	Epoch	$M_{\rm U}$	$A_{\rm U}$	$M_{\rm B}$	$A_{\rm B}$	$M_{\rm V}$	$A_{\rm V}$	$M_{\rm R}$	$A_{\rm R}$
67	1991.37	8.299(.002)	0.0512(.0075)	7.984(.002)	0.0438(.0065)	7.214(.002)	0.0376(.0072)		
68	1991.37	8.310(.003)	0.0489(.0071)	7.995(.001)	0.0493(.0036)	7.2066(.0008)	0.0436(.0023)	6.524(.002)	0.0419(.0040)
69	1991.40	8.298(.003)	0.0535(.0092)	7.992(.002)	0.0613(.0059)	7.204(.001)	0.0493(.0042)		
70	1991.45	8.312(.004)	0.0404(.0100)	7.989(.002)	0.0246(.0047)	7.215(.002)	0.0349(.0050)		
71	1991.47	8.307(.002)	0.0306(.0062)	7.986(.001)	0.0258(.0046)	7.201(.002)	0.0266(.0061)		
72	1991.49	8.321(.003)	0.0266(.0090)	7.992(.002)	0.0298(.0080)	7.193(.003)	0.047(.011)	6.543(.002)	0.0220(.0070)
73	1991.57	8.332(.003)	0.0383(.0085)	8.006(.003)	0.045(.010)	7.208(.003)	0.0348(.0098)	6.545(.002)	0.0242(.0083)
74	1991.66	8.319(.004)	0.036(.012)	8.009(.002)	0.0254(.0054)	7.223(.002)	0.0231(.0070)	6.545(.002)	0.0198(.0049)
75	1991.76	8.327(.002)	0.0616(.0097)	8.022(.002)	0.0476(.0074)	7.228(.002)	0.0299(.0052)	6.559(.003)	0.0348(.0079)
76	1991.76			7.991(.002)	0.0275(.0058)	7.204(.002)	0.0268(.0056)		
78	1991.83	8.336(.003)	0.045(.011)	8.031(.002)	0.0539(.0058)	7.238(.001)	0.0449(.0049)	6.5661(.0007)	0.0404(.0028)
79	1991.83			8.006(.002)	0.0332(.0062)	7.214(.002)	0.0338(.0054)		
80	1992.38			7.979(.003)	0.1221(.0064)	7.191(.003)	0.1071(.0085)		
82	1992.47			7.973(.003)	0.1549(.0082)	7.188(.001)	0.1293(.0034)		
83	1992.57	8.313(.004)	0.196(.012)	8.009(.002)	0.1749(.0064)	7.218(.002)	0.1470(.0049)	6.536(.002)	0.1196(.0048)
85	1992.67	8.312(.005)	0.153(.016)	8.003(.004)	0.1313(.0098)	7.208(.002)	0.0940(.0069)	6.531(.002)	0.0794(.0060)
87	1992.75	8.299(.004)	0.154(.015)	7.985(.003)	0.1015(.0073)	7.202(.002)	0.0724(.0061)	6.520(.002)	0.0560(.0062)
88	1992.77	8.295(.003)	0.1415(.0096)	7.967(.002)	0.1088(.0052)	7.174(.002)	0.0797(.0041)		
89	1992.83			8.001(.002)	0.1411(.0060)	7.211(.002)	0.1111(.0052)	6.531(.004)	0.0921(.0096)
90	1992.87	8.308(.007)	0.113(.018)	7.965(.003)	0.0811(.0054)	7.179(.003)	0.0933(.0098)		
92	1993.43	8.265(.001)	0.1205(.0043)	7.945(.002)	0.1040(.0061)	7.155(.002)	0.0765(.0050)		
93	1993.45	8.255(.010)	0.151(.030)	7.961(.003)	0.1126(.0094)	7.182(.002)	0.0769(.0051)	6.505(.002)	0.0587(.0059)
94	1993.54	8.249(.003)	0.1363(.0084)	7.954(.002)	0.1212(.0048)	7.173(.001)	0.0889(.0042)	6.499(.002)	0.0728(.0045)
97	1993.61	8.249(.004)	0.153(.015)	7.953(.002)	0.1111(.0084)	7.177(.002)	0.0898(.0055)	6.500(.001)	0.0761(.0041)
99	1993.68	8.269(.005)	0.138(.013)	7.956(.001)	0.1247(.0036)	7.175(.002)	0.1074(.0054)	6.503(.002)	0.0881(.0049)
100	1993.71	8.255(.004)	0.136(.012)	7.932(.002)	0.1115(.0062)	7.147(.002)	0.0949(.0046)		
103	1993.78	8.271(.002)	0.1251(.0066)	7.970(.002)	0.0679(.0051)	7.190(.002)	0.0569(.0047)	6.509(.002)	0.0611(.0069)
104	1993.81	8.279(.002)	0.0805(.0070)	7.9409(.0010)	0.0690(.0030)	7.159(.002)	0.0553(.0055)		
105	1993.90	8.303(.006)	0.080(.019)	7.960(.001)	0.0616(.0044)	7.172(.003)	0.0624(.0091)		
106	1994.48	8.303(.006)	0.062(.019)	7.962(.002)	0.0556(.0075)	7.172(.002)	0.0665(.0061)		
107	1994.48			8.003(.002)	0.0528(.0060)	7.212(.002)	0.0479(.0059)	6.527(.002)	0.0423(.0044)
108	1994.55	8.301(.003)	0.059(.014)	8.002(.002)	0.0411(.0071)	7.213(.003)	0.0592(.0076)	6.530(.002)	0.0455(.0060)
109	1994.63	8.325(.005)	0.073(.016)	8.015(.002)	0.0602(.0057)	7.225(.002)	0.0640(.0077)	6.541(.002)	0.0550(.0048)
110	1994.70	8.320(.003)	0.114(.011)	8.011(.002)	0.0725(.0076)	7.216(.002)	0.0674(.0064)	6.536(.002)	0.0659(.0085)
111	1995.48	8.322(.003)	0.1389(.0084)	8.013(.002)	0.1274(.0054)	7.208(.002)	0.1057(.0061)		
112	1995.75	8.336(.005)	0.169(.016)	8.001(.002)	0.1313(.0054)	7.197(.003)	0.1063(.0078)		
113	1995.83	8.353(.006)	0.091(.018)	8.008(.003)	0.078(.011)	7.195(.001)	0.0583(.0045)		
114	1995.90	8.350(.004)	0.0196(.0096)	8.009(.001)	0.0141(.0030)	7.199(.001)	0.0252(.0036)		

$M_{\rm V}$ has varied between 7.10 (SET=23) and 7.26 (SET=10), and $A_{\rm V}$ from 0.01 (SET=14) to 0.24 (SET=45). There has been a half a year interval of nearly constant brightness (Fig. 1: SET=67–79), as well as changes from high $A_{\rm V}$ to nearly constant brightness during a few months (e.g. Fig. 1: SET=112–114). Contrary to $A_{\rm V}$, the $M_{\rm V}$ changes are smoother, but with some scatter superimposed. This may be partly due to photometric transformation inaccuracies for the data from different observatories. Nevertheless, this short–term $M_{\rm V}$ scatter is mostly intrinsic to the object, because consecutive light curves are continuous (Fig. 1). The surface temperature of V 1794 Cyg follows these long–term mean brightness changes, since $M_{\rm B}-M_{\rm V}$ decreases when the brightness increases (Fig. 3c).

A second order weighted TSPA was performed for the $M_{\rm B}$, $M_{\rm V}$, $A_{\rm B}$ and $A_{\rm V}$ changes (Paper I: $K=2$ in Eq. 1). The best $M_{\rm V}$ periods were $P_{\rm cycle}=15^{\rm y}.0\pm0.^{\rm y}6$ and $7.^{\rm y}3\pm0.^{\rm y}3$. Correlation between $M_{\rm B}$ and $M_{\rm V}$ (Figs. 3ab) induced the same periodicities for the former. The first $P_{\rm cycle}=15^{\rm y}$ ($\sim$ double sinusoid) represents the whole data time span without the "lonely" $M_{\rm V}$ at 1975. The second $P_{\rm cycle}=7.^{\rm y}3$ ($\sim$ sinusoid) is about $15^{\rm y}/2$. Both $P_{\rm cycle}$ are not significant, because the 93 values of $M_{\rm V}\pm\sigma_{\rm M_V}$ have $\chi^2_0\approx 8000$ (Eq. 10 in Paper I: $P(\chi^2_0)=1$). Our $\sigma_{\rm M_V}$ in Table 1 are comparable to photometric internal accuracies $\sigma_{\rm int}\approx0.^{\rm m}003$. These $M_{\rm V}$ periodicities would not be significant even if the external accuracy ($\sigma_{\rm ext}\approx0.^{\rm m}015$) were assumed to reduce the χ^2_0 by $\sigma^2_{\rm int}(\sigma^2_{\rm int}+\sigma^2_{\rm ext})^{-1}\approx0.17$, i.e. from $\chi^2_0=8000$ to $\sim 140>n=93$. The short–term $M_{\rm V}$ changes are therefore real, because $P_{\rm cycle}=15^{\rm y}$ represents the whole observing interval without the $M_{\rm V}$ value at 1975. A significant second order $P_{\rm cycle}=15^{\rm y}$ model would require a much more conservative

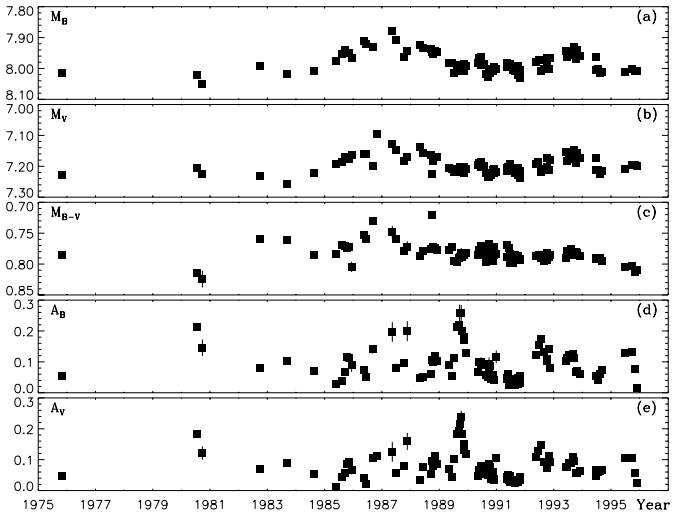

Fig. 3a–e. The $M_{\rm B}$, $M_{\rm V}$, $M_{\rm B}-M_{\rm V}$, $A_{\rm B}$ and $A_{\rm V}$ changes (Table 1)

$\sigma_{\rm ext}$ than our $0.^{\rm m}015$. The $A_{\rm B}$ and $A_{\rm V}$ changes are neither periodic. The best $P_{\rm cycle}=2.^{\rm y}62\pm0.^{\rm y}03$ for $A_{\rm V}$ has $\chi^2_0\approx2000$ for $n=93$. And here $\sigma_{\rm ext}$ does not influence χ^2_0, because the $A_{\rm V}$ are nearly independent of external accuracy. Thus we can not reject the "null hypothesis" that the $A_{\rm V}$ variations are pure noise (Paper I: H_0 in Sect. 3.3). In conclusion, V 1794 Cyg has no regular M or A cycles.

The earlier M and A periodicities were detected with the power spectrum method from data between 1975 and 1989 (Jetsu et al. 1990a, 1990b). Those studies relied on a constant P ephemeris with a sinusoidal model. Without the first two subsets in Jetsu et al. (1990a, 1990b), the others were between 1980 and 1989, which explains this earlier $9.^{\rm y}1$ cycle detection for M. The significance of the other $2.^{\rm y}8$ cycle in A was not estimated in Jetsu et al. (1990a, 1990b), but here $P_{\rm cycle}=2.^{\rm y}62$ for $A_{\rm V}$ must certainly be rejected.

4. Normalized magnitudes

In this section the three stage period analysis (TSPA) from Paper I is applied to the $\bar{y}_{\rm norm}$ of V 1794 Cyg. The 21 subsets with less than 7 nights of observations were not normalized, and subsequently not analysed with the TSPA. Table 3 gives the P, $t_{\rm min,1}$ and $t_{\rm min,2}$ for the remaining 93 subsets with $\rm nts\geq7$. Paper I summarized three rules for rejecting some P, $t_{\rm min,1}$ or $t_{\rm min,2}$ estimates. The *first* rule rejected the P, $t_{\rm min,1}$ and $t_{\rm min,2}$ of a SET, if the bootstrap distribution of any model parameter was not gaussian (Paper I: $\rm R_I$). Two detailed TSPA analysis examples for the subsets SET=42 and 114 were presented in Paper I. When we performed the same TSPA analysis procedures for each of the 93 subsets of normalized photometry, the $\rm R_I$ rejection rates were 5/12 and 8/81 for $\rm nts<10$ and $\rm nts\geq10$ subsets, i.e. more data increased modelling reliability. These thirteen $\rm R_I$ rejections are indicated by "r" in column $H_{\rm G}$ of Table 3. Thus our *second* rule (Paper I: $\rm R_{II}$) rejected the P, $t_{\rm min,1}$ and $t_{\rm min,2}$ of every $\rm nts<10$ subset (Table 3: 12/93 subsets). Finally, the *third* rule rejected nine "unreal" $t_{\rm min,2}$ in Table 3, which were those not present in $S\geq190$ bootstrap samples out of 200 (Paper I: $\rm R_{III}$). A detailed $\rm R_I$ and $\rm R_{III}$ rejection example for SET=114 was given in Paper I (Sect. 6.2). Our Table 3 also contains all rejected P, $t_{\rm min,1}$ and $t_{\rm min,2}$, because these undoubtedly contain some, although less reliable, TSPA modelling information.

Table 2. The best P detected for $T_{\rm i}$ with the SD–, WSD–, K– and WK–methods. The critical levels for the P detected with the nonweighted SD– and K–methods are $Q_{\rm SD}$ and $Q_{\rm K}$ (Paper III: Eqs. 19 and 24)

	SD–method		WSD–method
	P	$Q_{\rm SD}$	P
best	3.2811 ± 0.0010	0.0086	3.2812 ± 0.0010
2nd best	3.3194 ± 0.0011	0.017	3.2851 ± 0.0010
	K–method		WK–method
	P	$Q_{\rm K}$	P
best	3.3175 ± 0.0011	0.0029	3.28020 ± 0.00076
2nd best	3.28836 ± 0.00068	0.0042	3.32158 ± 0.00094

4.1. Active longitudes: the $t_{\rm min,1}$ and $t_{\rm min,2}$ changes

Numerous studies have uncovered active longitudes in chromospherically active stars (e.g. Eaton & Hall 1979; Hall 1987, 1991; Zeilik 1991; Jetsu 1996). The starspots seem to concentrate on such long–lived regions rotating with a constant angular velocity. Here the active longitudes of V 1794 Cyg are searched for in the $t_{\rm min,1}$ and $t_{\rm min,2}$ epochs using the nonparametric methods from Jetsu & Pelt (1996: Paper III). Active longitudes were detected in four RS CVn binaries with these methods in Jetsu (1996), where the data were the epochs when the starspots modelled by Henry et al. (1995) crossed the centre of the visible stellar disk. Here the data ($T_{\rm i}\pm\sigma_{\rm T_i}$) are the $t_{\rm min,1}$ and $t_{\rm min,2}$ not rejected with $\rm R_I$, $\rm R_{II}$ and $\rm R_{III}$ (Table 3: $n=81$). These $T_{\rm i}$ are circular data when folded with an arbitrary P. We searched for periodicity in $T_{\rm i}$ with the nonparametric methods by Kuiper (1960: the K–method) and Swanepoel & DeBeer (1990: the SD–method), and their weighted versions that can also utilize $\sigma_{\rm T_i}$ (Paper III: the WK– and WSD–methods). These methods test the "null hypothesis" ($H_{\rm P}$): "*The $\phi_{\rm T_i}$ of $T_{\rm i}$ with an arbitrary P are randomly distributed between 0 and 1.*" We tested $H_{\rm P}$ between $P_{\rm min}=3.^{\rm d}15$ and $P_{\rm max}=3.^{\rm d}45$, i.e. within $\pm5\%$ from $(P_{\rm max}-P_{\rm min})/2=3.^{\rm d}30$. As in Jetsu (1996), the significance level for rejecting $H_{\rm P}$ was $\gamma=0.001$. The best $P_{\rm SD}=3.2811\pm0.0010$ and $P_{\rm K}=3.3175\pm0.0011$ had critical levels $Q_{\rm SD}=0.0086$ and $Q_{\rm K}=0.0029>\gamma=0.001$ (Table 2). Hence $H_{\rm P}$ was not rejected for V 1794 Cyg.

The $T_{\rm i}\pm\sigma_{\rm T_i}$ data quality prevented $Q_{\rm WSD}$ and $Q_{\rm WK}$ estimates with the weighted WSD– and WK–methods. The two largest rescaled $T_{\rm i}$ weights (Jetsu 1996: $w_{\rm i}$ in Eq. 1) are $w_{\rm max,1}=w_{\rm max,2}=4.65$, the smallest being $w_{\rm min,1}=0.04$. The ratio $W_{\rm R}=w_{\rm max,1}/w_{\rm min}=108.5$ exceeds those in Jetsu (1996: Table 1), while the WSD–method "breakdown" parameter is $R(s)=0.04$ (Jetsu 1996: Eq. 5). Both $R(s)$ and $W_{\rm R}$ indicate unreliable $Q_{\rm WSD}$ and $Q_{\rm WK}$ estimates. However, the order of

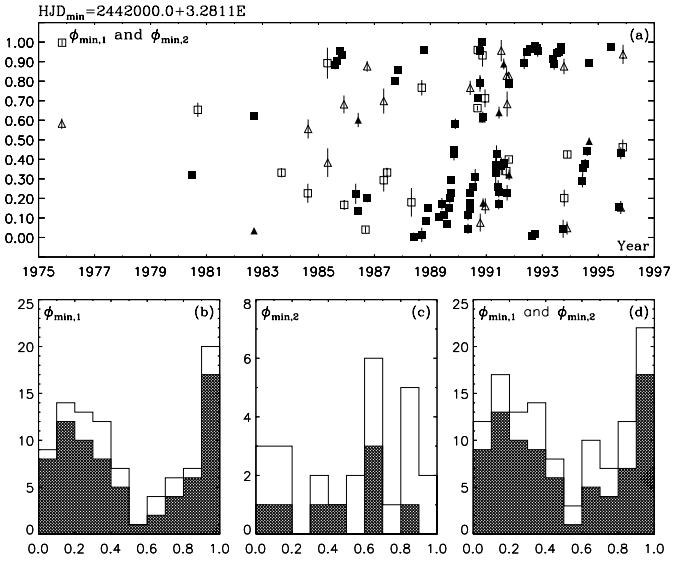

Fig. 4. a The primary and secondary minima phases ($\phi_{\min,1}$, $\phi_{\min,2}$) with $\mathrm{HJD_{min}} = 2442000.0 + 3.2811\mathrm{E}$. The rules $\mathrm{R_I}$, $\mathrm{R_{II}}$ or $\mathrm{R_{III}}$ for rejecting/not rejecting some of these $\phi_{\min,1}$ and $\phi_{\min,2}$ estimates are explained in the beginning of Sect. 4. The $\phi_{\min,1}$ and $\phi_{\min,2}$ rejected/not rejected with $\mathrm{R_I}$, $\mathrm{R_{II}}$ or $\mathrm{R_{III}}$ are denoted with open/closed squares and open/closed triangles, respectively. **b** White/dark distributions denote $\phi_{\min,1}$ rejected/not rejected with $\mathrm{R_I}$, $\mathrm{R_{II}}$ or $\mathrm{R_{III}}$. **c** As in **b** for $\phi_{\min,2}$. **d** Combined $\phi_{\min,1}$ and $\phi_{\min,2}$ distributions

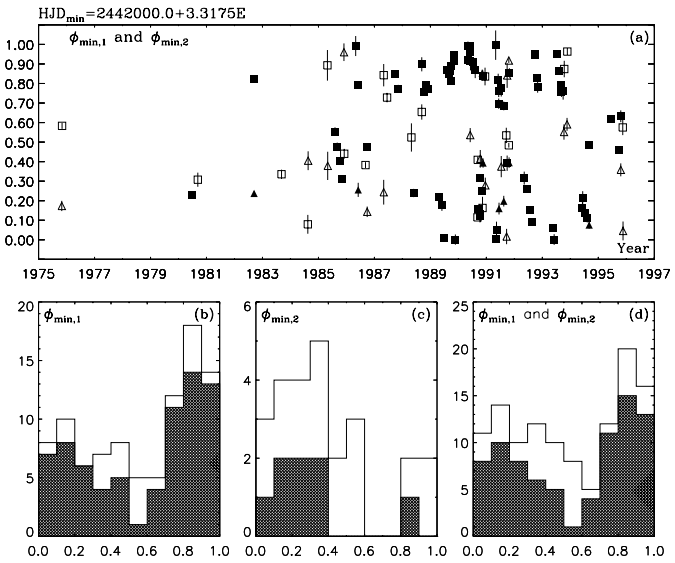

Fig. 5a–d. As in Fig. 4 for $\mathrm{HJD_{min}} = 2442000.0 + 3.3175\mathrm{E}$

significance and the σ_{P} estimates for the P detected with these weighted methods are correct in Table 2 (see Paper III: Sect. 5).

No significant active longitudes were detected for V 1794 Cyg, unlike in an equivalent analysis for four RS CVn binaries (Jetsu 1996). This absence of T_{i} periodicity verifies the inappropriateness of a traditional constant P ephemeris for V 1794 Cyg. Several phenomena complicate active longitude detection, strong differential rotation being the most probable one (Sect. 4.2). V 1794 Cyg had several low amplitude light curves with inaccurate $t_{\min,1}$ and $t_{\min,2}$. The SD– and K–

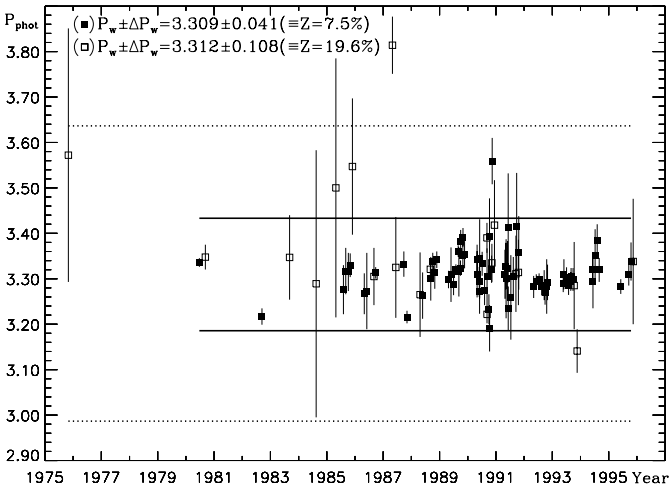

Fig. 6. P rejected (open squares) and not rejected (closed squares) with $\mathrm{R_I}$ and $\mathrm{R_{II}}$ (Table 3: $\pm 3\sigma_{\mathrm{P}}$ errors!). The dotted and continuous horizontal lines are the respective $P_{\mathrm{w}} \pm 3\Delta P_{\mathrm{w}}$ limits

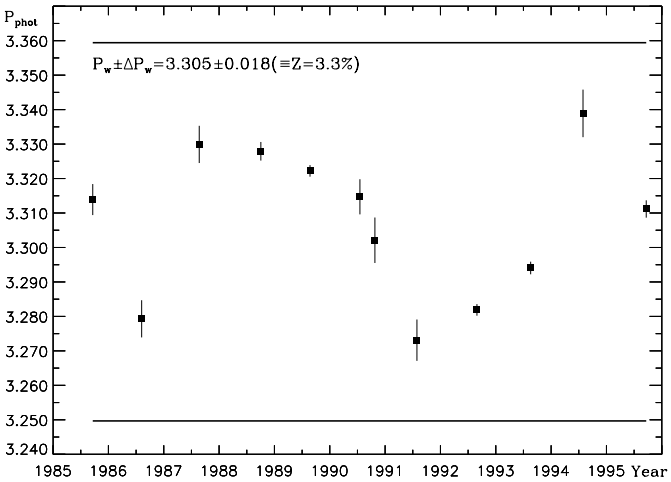

Fig. 7. P for the yearly $\bar{y}_{\mathrm{norm}}$ (Table 4: $\pm 3\sigma_{\mathrm{P}}$ errors!). Note the two P values in 1990 when the only observed abrupt phase shift of ~ 0.5 occurs

methods analyse all T_{i} with unity weights. Hence these low amplitude light curves deteriorate the T_{i} statistics. Because $\mathrm{R_I}$, $\mathrm{R_{II}}$ and $\mathrm{R_{III}}$ already eliminate a sizeable fraction of data, an additional rule would have been questionable (e.g. rejecting T_{i} when A_{V} goes below some fixed limit). On the other hand, no quantitative significance estimates for the active longitudes in chromospherically active stars have been published, except for those given here and in Jetsu (1996). For example, Eaton & Hall (1979), Hall (1987, 1991) or Zeilik (1991) do not quantify the statistics of this phenomenon. This may justify our subsequent *qualitative* $\phi_{\mathrm{T_i}}$ study with the best P_{WK} and P_{SD} of Table 2, not forgetting that these periodicities do not reach $\gamma = 0.001$.

Although $P_{\mathrm{K}} = 3.3175$ has the best critical level ($Q_{\mathrm{K}} < Q_{\mathrm{SD}}$), the $\phi_{\mathrm{T_i}}$ with $P_{\mathrm{SD}} = 3.2811$ are discussed first, this periodicity being within $\pm 1\sigma_{\mathrm{P}}$ the best one detected with the SD–, WSD– and WK–methods (Table 2). Fig. 4 displays the $\phi_{\mathrm{T_i}}$ with $P_{\mathrm{SD}} = 3.2811$ and an arbitrary zero epoch. The long–term $\phi_{\mathrm{T_i}}$

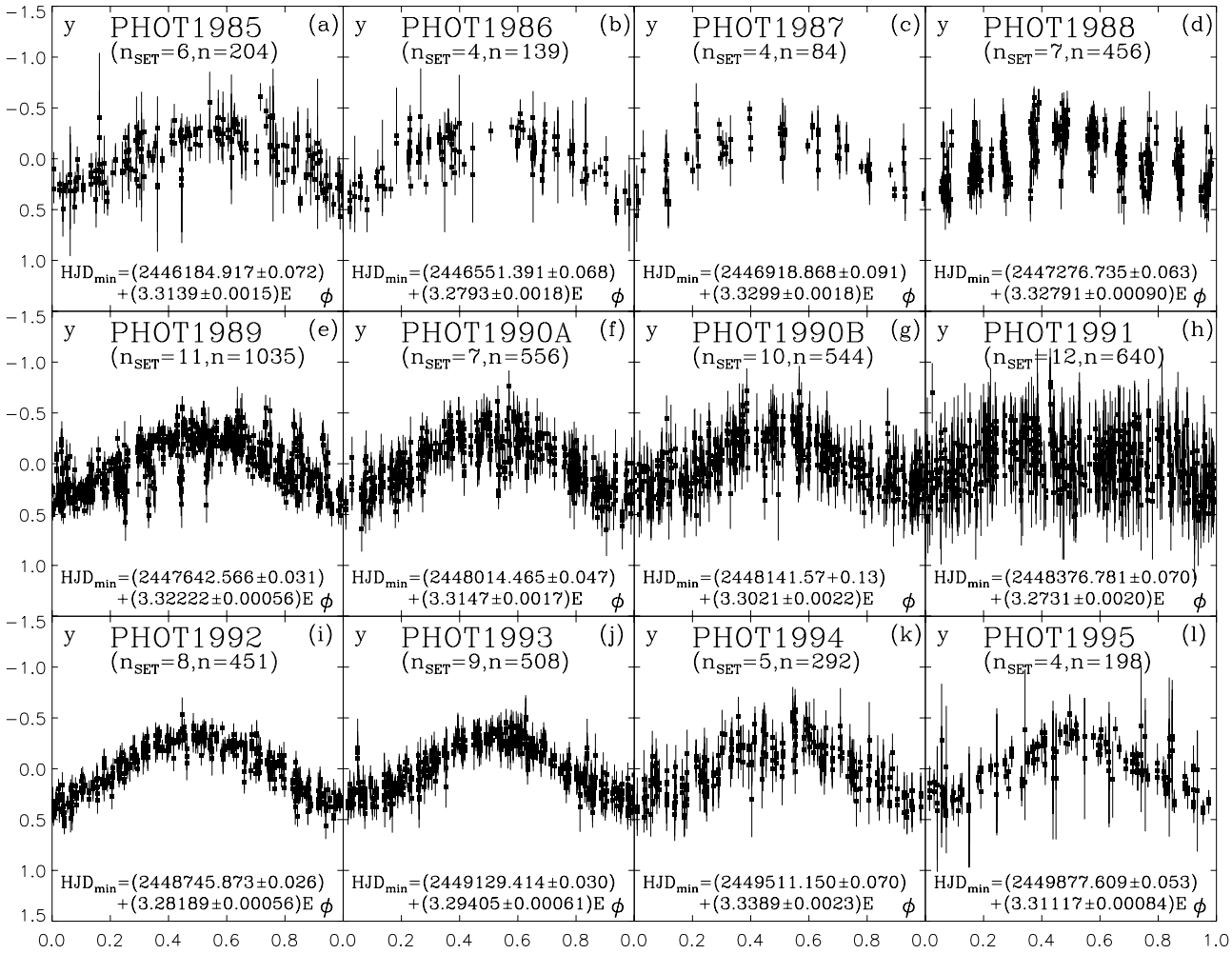

Fig. 8. The n yearly $\bar{y}_{\rm norm}$ for $n_{\rm SET}$ subsets and their ephemerides. Note that 1990 is divided into PHOT1990A and PHOT1990B

changes appear irregular, and even the yearly changes are rapid (Fig. 4a). Note that the dark and white distributions denote the analysed and rejected $\phi_{\rm T_i}$, respectively. The dark $\phi_{\rm min,1}$ distribution is broad and unimodal, the white rejected one being uniform, i.e. random (Fig. 4b). The dark and white $t_{\rm min,2}$ distributions are nearly uniform (Fig. 4c). The combined dark unimodal $\phi_{\rm min,1}$ and $\phi_{\rm min,2}$ distribution is too dispersed to reach $\gamma = 0.001$.

A similar discussion is unnecessary for $P_{\rm K} = 3.3175$, but some striking features in Fig. 5 deserve a few comments. The $\phi_{\rm min,1}$ and $\phi_{\rm min,2}$ distributions are similar (Fig. 5bc). Furthermore, the rejected/not rejected distributions resemble each other, especially for $\phi_{\rm min,2}$. Although the rejected data were not analysed, they fit the analysed data. Thus $P_{\rm K} = 3.3175$ might represent a real structure having rotated with a constant angular velocity for about two decades. After all, the dark distribution in Fig. 5d is quite improbable ($Q_{\rm K} = 0.0029$). Finally, Figs. 4 and 5 connect through $(P_{\rm SD}^{-1} + P_{\rm K}^{-1})^{-1} = 299^{\rm d} \pm 12^{\rm d}$, which is relatively close to the $365^{\rm d}$ window. But is $P_{\rm SD}$ or $P_{\rm K}$ "real" or "spurious", remains unsolved. In conclusion, the active longitudes of V 1794 Cyg are a controversial subject, although we reject this hypothesis with $\gamma = 0.001$.

4.2. Differential rotation: the P changes

The short–term P changes indicate detectable differential rotation in V 1794 Cyg. Fig. 6 displays the rejected and nonrejected P from Table 3 with $\pm 3\sigma_{\rm P}$ errors. Their respective weighted means, $P_{\rm w} \pm \Delta P_{\rm w} = 3.312 \pm 0.108$ and 3.309 ± 0.041, give $Z = 6 \Delta P_{\rm w} P_{\rm w}^{-1} = 19.6\%$ and 7.5% (Jetsu et al. 1993: Eq. 3). These Z confirm that a reliable TSPA requires $\rm nts \geq 10$. Nevertheless, even $Z = 7.5\%$ implies three times stronger differential rotation in V 1794 Cyg than in FK Com (Jetsu et al. 1993: $Z = 2.4\%$). These rapid irregular P changes interfere with active longitude detection and verify the uselessness of a constant P ephemeris. The detailed example for SET=114 with nts=16 revealed that $\rm nts \geq 10$ by itself is not a sufficient condition for a reliable TSPA (Paper I: Sect. 6.2). The TSPA of low amplitude light curves is especially unstable, e.g. the P difference certainly exceeds $\pm 1\sigma_{\rm P}$ for the simultaneous SET=61 and 62 (nts=16 and 23). Since P is unique in time, these data must contain unidentified errors.

Latitude does not determine the angular velocity of an individual sunspot. One should not forget the "sobering reminder" about the solar differential rotation law (Howard 1994: his

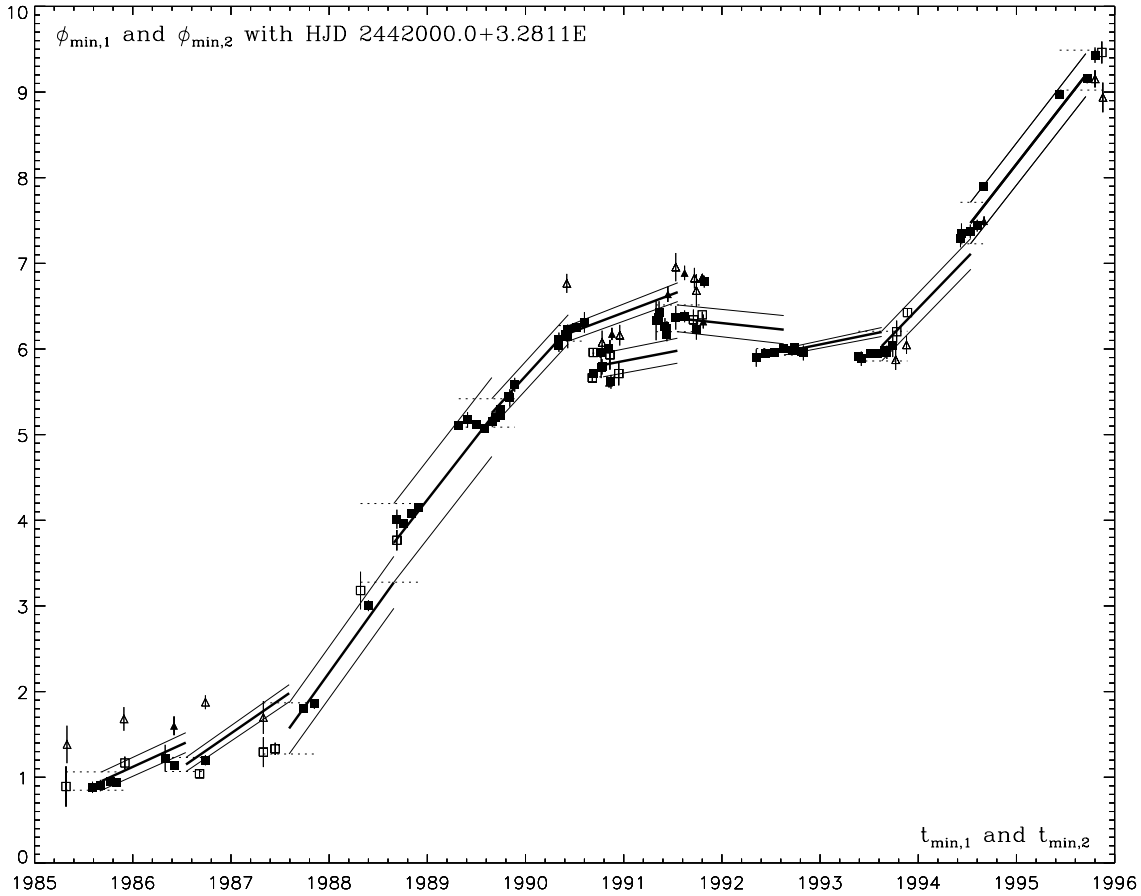

Fig. 9. The predictions for the yearly means of the primary minima $\phi_{\min,1}$ from Table 4. The beginning of Sect. 4.3. contains a detailed example of how the yearly P of PHOT1985 and PHOT1986 provide one of these predictions. The $\phi_{\min,1}$ and $\phi_{\min,2}$ rejected/not rejected with R_I, R_{II} and R_{III} are denoted by open/closed squares and open/closed triangles, respectively. The horizontal dashed lines are the yearly $\langle\phi_{\min,1}\rangle_{\rm obs}\pm\sigma_{\phi,\rm obs}$ limits. The $\Delta\phi$ path (thick continuous line) connects earlier observed yearly $(\langle t\rangle, \langle\phi_{\min,1}\rangle_{\rm obs})$ to the predicted ones $(\langle t\rangle, \langle\phi_{\min,1}\rangle_{\rm pred})$. The narrow continuous lines denote the error limits $\langle\phi_{\min,1}\rangle_{\rm pred} \pm 1\sigma_{\phi,\rm pred}$. Note that 1990 consists of PHOT1990A and PHOT1990B

Fig. 2). This law, frequently cited in connection with stellar differential rotation (e.g. Hall & Busby 1990: Eq. 2), relies on a gigantic sample (e.g. Howard 1994: 36708 sunspot groups). Were the solar–stellar–connection literally valid, regular P changes would be hard to detect in the meagre stellar data samples. Does our empirical Fig. 6 then support this conclusion? Suppose a stellar counterpart for the solar butterfly diagram, where the latitude of main activity correlates with the starspot cycle phase. This might be detectable as regular yearly P changes, assuming no abrupt longitudinal shifts for the activity centres. Fig. 7 displays the P obtained with TSPA for the yearly $\bar{y}_{\rm norm}$. This analysis was restricted between 1985 and 1995, because at least four $\bar{y}_{\rm norm}$ subsets per year ($n_{\rm SET}$) were available during this interval. Fig. 8 shows the $\bar{y}_{\rm norm}$ with these yearly ephemerides. Their predictability, as well as the two ephemerides for 1990, are the subject of our next Sect. 4.3.

Unlike the seasonal (Fig. 6), the yearly P changes are surprisingly regular (Fig. 7). These P are very accurate (Fig. 7: $P\pm3\sigma_{\rm P}$), and might even follow some cycle, except for those at 1986 and 1994. They fulfill $Z = 3.3\%$ with $P_{\rm w} = 3.305$, and suggest that our nonparametric $T_{\rm i}$ analysis in Sect. 4.1 could have been restricted within $\pm1.65\%$ ($\equiv Z/2$) around 3.30. These yearly P might represent the butterfly diagram of V 1794 Cyg, but reveal no significant correlation with M. Again a solar analogy could explain this, because the sunspot maximum coincides with the main activity on the butterfly diagram mid–latitudes. This could induce a phase shift of several years between P and M. But V 1794 Cyg has had only one well established M minimum at 1991 (i.e. spot maximum), and two uncertain ones at 1984 and 1994 (Fig. 3). Hence we do not speculate about the connection between these regular yearly P changes, and latitudinal migration or activity cycle (if there is any).

4.3. Migration

The yearly P gave the $\bar{y}_{\rm norm}$ ephemerides in Fig. 8. Although the inadequacy of a constant P ephemeris for the *whole* data has been frequently emphasized, this does not necessarily indicate disruption for the regions of main activity. For example, latitudinal migration might induce apparent disruption. The $t_{\min,1}$ modulations for the very same long–lived active region could resemble the continuous O–C changes of the primary and

Table 3. The $t_{\min,1}$, $t_{\min,2}$ and P for the $\bar{y}_{\rm norm}$ of subsets with $\mathrm{nts} \geq 7$. The $\mathrm{R_I}$ rejections are denoted with "r" in column $H_{\rm G}$, while the $\mathrm{R_{II}}$ rejections are applied to subsets with $\mathrm{nts} < 10$. Finally, $\mathrm{R_{III}}$ rejects the $t_{\min,2}$ with $S < 190$

SET	nts	$H_{\rm G}$	P	$t_{\min,1}$	$t_{\min,2}$ (S)	SET	nts	$H_{\rm G}$	P	$t_{\min,1}$	$t_{\min,2}$ (S)
1	7	r	3.572±.093	42721.832±.051	42720.472±.087(197)	62	23		3.191±.017	48180.91±.10	48178.56±.15(128)
3	14		3.3358±.0032	44419.214±.041		63	17		3.321±.010	48204.559±.061	48206.553±.061(200)
4	9	r	3.3477±.0091	44495.78±.12		64	16	r	3.335±.014	48210.90±.19	
6	10		3.2169±.0060	45230.651±.024	45228.715±.034(200)	65	14		3.559±.017	48213.148±.089	48214.981±.079(200)
10	8		3.347±.031	45587.330±.078		66	11	r	3.418±.033	48242.99±.15	48244.46±.13(200)
12	9		3.289±.098	45931.50±.16	45932.58±.16(149)	67	15		3.310±.018	48379.54±.25	
14	8	r	3.500±.095	46186.33±.26	46187.94±.24(200)	68	11		3.328±.017	48389.521±.047	
15	16		3.276±.018	46284.731±.071		69	17		3.300±.029	48392.99±.14	
16	20		3.317±.017	46314.329±.071		70	19		3.323±.020	48412.12±.11	
17	17		3.315±.014	46350.586±.043		71	14		3.412±.040	48421.884±.098	
18	13		3.3298±.0087	46373.498±.035		72	16		3.235±.016	48421.674±.087	48423.21±.10(200)
19	13	r	3.547±.050	46403.783±.083	46402.19±.15(196)	73	26		3.259±.031	48455.12±.15	48453.78±.18(186)
20	12		3.267±.015	46554.90±.17		74	27		3.306±.014	48487.985±.074	48486.368±.091(200)
21	12		3.273±.028	46587.416±.052	46588.95±.12(192)	75	11	r	3.311±.028	48520.66±.13	48522.26±.13(200)
22	7		3.305±.021	46682.261±.050		76	18		3.416±.039	48530.14±.13	48531.63±.21(114)
23	13		3.3130±.0042	46702.472±.065	46704.690±.089(154)	78	12	r	3.314±.024	48553.667±.039	48551.789±.041(200)
24	9	r	3.814±.021	46919.33±.19	46920.66±.21(197)	79	15		3.357±.027	48558.218±.075	48556.690±.089(200)
25	10	r	3.325±.037	46965.395±.080		80	13		3.2820±.0081	48752.16±.11	
27	13		3.3323±.0093	47068.644±.046		82	21		3.2943±.0052	48785.153±.055	
29	10		3.2158±.0046	47108.201±.062		83	28		3.2981±.0046	48821.290±.025	
30	16	r	3.265±.031	47279.88±.24		85	23		3.2822±.0063	48854.250±.046	
31	12		3.263±.017	47312.112±.070		87	18		3.286±.011	48886.958±.049	
32	7		3.3209±.0073	47416.33±.13		88	17		3.2700±.0090	48896.923±.033	
33	20		3.300±.016	47417.14±.12		89	11		3.283±.020	48919.743±.052	
34	14		3.3383±.0063	47443.216±.037		90	11		3.292±.013	48929.533±.095	
35	17		3.314±.012	47469.863±.041		92	23		3.2901±.0065	49132.820±.059	
36	18		3.3419±.0061	47496.336±.033		93	14		3.310±.011	49142.582±.091	
37	15		3.2984±.0064	47647.114±.046		94	21		3.3022±.0077	49175.587±.033	
39	14		3.309±.020	47680.149±.098		97	18		3.2854±.0070	49201.849±.030	
40	26		3.2864±.0075	47712.769±.044		99	20		3.2941±.0069	49231.469±.045	
41	28		3.3201±.0039	47742.153±.031		100	18		3.3045±.0064	49237.980±.086	
42	22		3.3610±.0042	47771.943±.024		103	16		3.2984±.0084	49261.22±.15	
43	11		3.315±.018	47781.956±.088		104	9	r	3.285±.032	49274.86±.14	49273.79±.13(193)
44	12		3.3236±.0056	47801.948±.051		105	9		3.141±.016	49314.966±.055	49313.73±.11(182)
45	13		3.3820±.0085	47805.005±.041		106	15		3.321±.011	49514.67±.11	
46	15		3.3502±.0085	47831.984±.027		107	20		3.295±.020	49518.16±.12	
47	13		3.3914±.0068	47835.20±.11		108	21		3.352±.019	49547.762±.086	
48	11		3.353±.010	47855.391±.087		109	17		3.384±.012	49574.224±.077	
49	11		3.310±.017	48017.910±.084		110	14		3.3195±.0088	49598.678±.041	49600.643±.062(200)
50	11		3.342±.011	48017.684±.084		111	21		3.2829±.0054	49881.116±.038	
52	11		3.293±.011	48044.361±.048		112	21		3.3094±.0081	49983.428±.060	
53	11		3.271±.016	48051.099±.046	48049.58±.12(150)	113	16		3.338±.014	50013.86±.10	50012.95±.11(112)
54	20		3.344±.029	48050.83±.15		114	16	r	3.338±.046	50040.21±.14	50041.77±.19(163)
55	27		3.3330±.0088	48084.002±.053							
56	26		3.275±.011	48113.71 ± .13							
57	9		3.390±.011	48144.391 ± .041							
58	9		3.2217±.0066	48145.367 ± .051							
59	19		3.304±.021	48147.842 ± .049							
60	15		3.233±.011	48171.601 ± .062							
61	16		3.393±.028	48177.62 ± .14							

secondary minima of eclipsing binaries (e.g. Jetsu et al. 1997: AR Lac). Such lagging or running ahead of $t_{\min,1}$ with a constant P would only be more prominent in V 1794 Cyg, and could display phase shifts. Assuming yearly phase coherence, this problem resembles that in Jetsu et al. (1997), except that the predictive periods are known (i.e. $P_{\rm pred}$ below). All $t_{\min,1}$ and $t_{\min,2}$ from Table 3 were transformed into phases with the ephemeris of Fig. 4, where $P_0 \pm \sigma_{\mathrm{P_0}} = 3.2811 \pm 0.0010$. *Only* $t_{\min,1}$ were analysed, assuming that the main region of activity crosses the centre of the visible stellar disk at these epochs. Since the ephemerides in Fig. 8 relied on all available yearly $\bar{y}_{\rm norm}$, both rejected and not rejected $t_{\min,1}$ were studied, which ensured adequate yearly $\phi_{\min,1}$ data. We denote the yearly $t_{\min,1}$ averages with $\langle t \rangle$. Our prediction begins from the six $\phi_{\min,1}$ of PHOT1985 with an average $\langle \phi_{\min,1} \rangle_{\rm obs} \pm \sigma_{\phi,\rm obs} = 0.96 \pm 0.11$ (Table 4). The periods $P_1 = 3.3139 \pm 0.0015$ (PHOT1985) and

$P_2 = 3.2793 \pm 0.0018$ (PHOT1986) determine a predictive period $P_{\rm pred} \pm \sigma_{\rm P,pred} = (P_1 + P_2)/2 = 3.2966 \pm 0.0012$. The $\langle t \rangle$ difference $\Delta t = 312.^{\rm d}9$ between PHOT1985 and PHOT1986 predicts a phase shift of $\Delta\phi = \Delta t(P_0^{-1} - P_{\rm pred}^{-1}) = 0.44$, where $\sigma^2_{\Delta\phi} = (\Delta t)^2(\sigma^2_{\rm P_0} P_0^{-4} + \sigma^2_{\rm P,pred} P_{\rm pred}^{-4})$. Hence the PHOT1986 prediction is $\langle \phi_{\rm min,1} \rangle_{\rm pred} = \langle \phi_{\rm min,1} \rangle_{\rm obs} + \Delta t(P_0^{-1} - P_{\rm pred}^{-1}) = 0.96 + 0.44 = 1.40$, where $\sigma^2_{\phi,\rm pred} = \sigma^2_{\phi,\rm obs} + \sigma^2_{\Delta\phi}$. The observed $\langle \phi_{\rm min,1} \rangle_{\rm obs} = 1.15$ for PHOT1986 yields a prediction residual $\rm RES = | \langle \phi_{\rm min,1} \rangle_{\rm pred} - \langle \phi_{\rm min,1} \rangle_{\rm obs} | = 0.25$. Table 4 summarizes all predictions from 1985 to 1995. This unique $\phi_{\rm min,1}$ path determined by the $\rm RES \leq 0.5$ minimization rule is outlined in Fig. 9. The cases $\rm RES \sim 0.5$ are uncertain, e.g. RES=0.46 could be –0.54 or 1.46 (from PHOT1987 to PHOT1988). If $\rm RES \geq 0.25$ represents unpredictability, Table 4 contains 7/11 such cases. Thus these yearly predictions fail. Yet, the yearly $\bar{y}_{\rm norm}$ curves are continuous, the phase coherence for high amplitude light curves being excellent (Fig. 8). The $\bar{y}_{\rm norm}$ dispersion is largest in PHOT1991 when the brightness of V 1794 Cyg was nearly constant (Figs. 1 and 8h). Furthermore, the observed yearly $\phi_{\rm min,1}$ changes are discontinuous *only* once (PHOT1990A and PHOT1990B). All other $\phi_{\rm min,1}$ discontinuities coincide with observational gaps. Although these yearly $\phi_{\rm min,1}$ changes display complex shapes with $P_0 = 3.2811$, they retain continuity (e.g. Fig. 9: "s"-shape during PHOT1989).

The only *observed* abrupt longitudinal activity shift occurs between SET=56 and 57 on September, 1990 (about $180°$). Hence the predicted pairs were from PHOT1989 to PHOT1990A, from PHOT1990A to PHOT1991, and from PHOT1990B to PHOT1991 (Table 4 and Fig. 8). Because the other $\phi_{\rm min,1}$ discontinuities within observational gaps can not be verified, we conclude that *only one activity shift is observed in V 1794 Cyg*. Thus the identification of "new" starspots after observational gaps is not trivial with a constant P, e.g. in the linear approach by Henry et al. (1995: their Figs. 4, 9, 15 and 20). Whether the $t_{\rm min,1}$ changes in V 1794 Cyg resemble the continuous O–C changes of eclipsing binaries, remains unsolved. The analysis by Berdyugina & Tuominen (1998) reveals such continuous longitudinal migration in four RS CVn binaries. Such continuous longitudinal migration in chromospherically active stars would mean that activity centres are not frequently disrupted. This $t_{\rm min,1}$ continuity could be resolved with uninterrupted long–term photometry of an active star sufficiently close to $\delta = \pm 90°$, say permanently $40°$ above the horizon. An automated telescope at higher latitudes could perform this task.

5. Conclusions

The seasonal (SET) light curves of V 1794 Cyg were modelled with a second order Fourier function (Eq. 1). The $P = P_{\rm phot}$ were determined separately for each subset to enable untroubled modelling of two phenomena undoubtedly present in V 1794 Cyg: *differential rotation* and longitudinal shifts of activity centres, also referred to as longitudinal activity migration that is connected to the concept of *active longitudes*. Our rejection of the traditional constant period ephemeris approach eliminated unique phases for the whole data. Unique *phase* information could, however, be retrieved from the epochs of the primary and secondary minima in *time* ($t_{\rm min,1}$ and $t_{\rm min,2}$) that are nearly independent of the seasonal P (see Jetsu et 1993: Fig. 8). Some outliers were removed as *flares* before normalizing the UBVRI magnitudes and modelling. If some of these outliers do represent photometric flares, they are of short duration, and temporally unconnected to the seasonal light curve maxima. Earlier studies have indicated that photometric flares in evolved stars tend to occur close to the light curve maximum, but are rare events of short duration (e.g. Jetsu et al. 1993, Henry & Newsom 1996).

Significant *activity cycles* were not detected in the mean (M) and the total amplitude (A) of seasonal UBVRI light curves. The previously reported M ($9.^{\rm y}1$) and A ($2.^{\rm y}8$) cycles in Jetsu (1990a, 1990b) were not significant, the former cycle essentially represented the time span of those earlier data. The difficulties of cycle detection in chromospherically active stars could be explained with a plausible solar–stellar analogy, i.e. by considerable changes in the total sunspot number from one solar cycle to another. Apart from not being strictly periodic (i.e. predictable), the solar cycle has even faded for prolonged intervals, like the Maunder Minimum.

The normalized magnitudes ($\bar{y}_{\rm norm}$) utilize the combined information from all UBVRI magnitudes. The seasonal $t_{\rm min,1}$, $t_{\rm min,2}$ and P were modelled from $\bar{y}_{\rm norm}$ with the three stage period analysis method (Paper I: TSPA). The complementary methods identified spurious periodicities ($\sim 6.^{\rm d}66, 0.^{\rm d}77, ...$) and confirmed that the $P_{\rm phot}$ of V 1794 Cyg is indeed $\sim 3.^{\rm d}3$ (Paper I: Sect. 6.3.). Bootstrap provided all model parameter estimates, and their errors. All models violating reliable bootstrap statistics were consistently discarded, i.e. significant deviations of any model parameter distribution from a gaussian. Three rejection rules excluded unreliable $t_{\rm min,1}$, $t_{\rm min,2}$ and P estimates from further analysis (see Table 3).

Active longitudes were searched for in the most reliable $t_{\rm min,1}$ and $t_{\rm min,2}$ epochs that are circular data when folded with an arbitrary P. The nonparametric methods from Paper III detected no periodicities reaching a significance level of $\gamma = 0.001$ for rejecting the "null hypothesis" that the $\phi_{\rm min,1}$ and $\phi_{\rm min,2}$ represent a random sample drawn from a uniform phase distribution. The critical levels for the best periods $P_{\rm SD} = 3.^{\rm d}2811$ and $P_{\rm K} = 3.^{\rm d}3175$ were $Q_{\rm SD} = 0.0086$ and $Q_{\rm K} = 0.0029$ (Table 2). The latter periodicity may represent an active longitude having rotated with a constant angular velocity for about two decades (Fig. 5).

If compared to the estimates in Hall & Busby (1990), the 7.5% variations of the most reliable seasonal P estimates would imply strong *differential rotation* in V 1794 Cyg (Fig. 6: closed squares). A lower 3.3% estimate was determined from the yearly $\bar{y}_{\rm norm}$ (Fig. 7). These regular yearly P changes did not correlate with those of M, and were therefore not interpreted as the "butterfly" diagram of V 1794 Cyg. As in the Sun, this absence of correlation between M and P might due to a phase shift of several years, the sunspot maximum coinciding with main activity on mid–latitudes, while at the sunspot minimum the activity

Table 4. The predicted $\phi_{\min,1}$ changes with $\mathrm{HJD_{min}} = 2442000.0 + 3.2811\mathrm{E}$. The $\langle t \rangle$, $P(t)$, $\langle \phi_{\min,1} \rangle_{\mathrm{obs}}$, Δt, P_{pred}, $\langle \phi_{\min,1} \rangle_{\mathrm{pred}}$ and RES parameters are explained Sect. 4.3

PHOT1985	$\langle t \rangle = 1985.68$	$P(t) = 3.3139 \pm 0.0015$	$\langle \phi_{\min,1} \rangle_{\mathrm{obs}} = 0.96 \pm 0.11$	
$\phi_{\min,1}$=0.89(SET=14)	$\phi_{\min,1}$=0.88(SET=15)	$\phi_{\min,1}$=0.90(SET=16)	$\phi_{\min,1}$=0.95(SET=17)	$\phi_{\min,1}$=0.94(SET=18)
$\phi_{\min,1}$=1.17(SET=19)				
PHOT1986 prediction:	$\Delta t = 312.9$	$P_{\mathrm{pred}} = 3.2966 \pm 0.0012$	$\langle \phi_{\min,1} \rangle_{\mathrm{pred}} = 1.40 \pm 0.12$	$\mathrm{RES} = 0.25$
PHOT1986	$\langle t \rangle = 1986.54$	$P(t) = 3.2793 \pm 0.0018$	$\langle \phi_{\min,1} \rangle_{\mathrm{obs}} = 1.15 \pm 0.08$	
$\phi_{\min,1}$=1.22(SET=20)	$\phi_{\min,1}$=1.13(SET=21)	$\phi_{\min,1}$=1.04(SET=22)	$\phi_{\min,1}$=1.20(SET=23)	
PHOT1987 prediction:	$\Delta t = 383.6$	$P_{\mathrm{pred}} = 3.3046 \pm 0.0013$	$\langle \phi_{\min,1} \rangle_{\mathrm{pred}} = 1.98 \pm 0.10$	$\mathrm{RES} = 0.41$
PHOT1987	$\langle t \rangle = 1987.59$	$P(t) = 3.3299 \pm 0.0018$	$\langle \phi_{\min,1} \rangle_{\mathrm{obs}} = 1.57 \pm 0.30$	
$\phi_{\min,1}$=1.29(SET=24)	$\phi_{\min,1}$=1.33(SET=25)	$\phi_{\min,1}$=1.80(SET=27)	$\phi_{\min,1}$=1.86(SET=29)	
PHOT1988 prediction:	$\Delta t = 389.6$	$P_{\mathrm{pred}} = 3.3289 \pm 0.0010$	$\langle \phi_{\min,1} \rangle_{\mathrm{pred}} = 3.28 \pm 0.30$	$\mathrm{RES} = 0.46$
PHOT1988	$\langle t \rangle = 1988.66$	$P(t) = 3.32791 \pm 0.00090$	$\langle \phi_{\min,1} \rangle_{\mathrm{obs}} = 3.74 \pm 0.46$	
$\phi_{\min,1}$=3.18(SET=30)	$\phi_{\min,1}$=3.00(SET=31)	$\phi_{\min,1}$=3.77(SET=32)	$\phi_{\min,1}$=4.01(SET=33)	$\phi_{\min,1}$=3.96(SET=34)
$\phi_{\min,1}$=4.08(SET=35)	$\phi_{\min,1}$=4.15(SET=36)			
PHOT1989 prediction:	$\Delta t = 364.6$	$P_{\mathrm{pred}} = 3.32507 \pm 0.00053$	$\langle \phi_{\min,1} \rangle_{\mathrm{pred}} = 5.21 \pm 0.46$	$\mathrm{RES} = 0.05$
PHOT1989	$\langle t \rangle = 1989.66$	$P(t) = 3.32222 \pm 0.00056$	$\langle \phi_{\min,1} \rangle_{\mathrm{obs}} = 5.25 \pm 0.17$	
$\phi_{\min,1}$=5.10(SET=37)	$\phi_{\min,1}$=5.17(SET=39)	$\phi_{\min,1}$=5.11(SET=40)	$\phi_{\min,1}$=5.07(SET=41)	$\phi_{\min,1}$=5.15(SET=42)
$\phi_{\min,1}$=5.20(SET=43)	$\phi_{\min,1}$=5.29(SET=44)	$\phi_{\min,1}$=5.22(SET=45)	$\phi_{\min,1}$=5.45(SET=46)	$\phi_{\min,1}$=5.43(SET=47)
$\phi_{\min,1}$=5.58(SET=48)				
PHOT1990A prediction:	$\Delta t = 284.6$	$P_{\mathrm{pred}} = 3.31846 \pm 0.00089$	$\langle \phi_{\min,1} \rangle_{\mathrm{pred}} = 6.23 \pm 0.17$	$\mathrm{RES} = 0.05$
PHOT1990A	$\langle t \rangle = 1990.44$	$P(t) = 3.3147 \pm 0.0017$	$\langle \phi_{\min,1} \rangle_{\mathrm{obs}} = 6.18 \pm 0.09$	
$\phi_{\min,1}$=6.04(SET=50)	$\phi_{\min,1}$=6.11(SET=49)	$\phi_{\min,1}$=6.17(SET=52)	$\phi_{\min,1}$=6.15(SET=54)	$\phi_{\min,1}$=6.23(SET=53)
$\phi_{\min,1}$=6.26(SET=55)	$\phi_{\min,1}$=6.31(SET=56)			
PHOT1991 prediction:	$\Delta t = 406.1$	$P_{\mathrm{pred}} = 3.2939 \pm 0.0013$	$\langle \phi_{\min,1} \rangle_{\mathrm{pred}} = 6.66 \pm 0.11$	$\mathrm{RES} = 0.31$
PHOT1990B	$\langle t \rangle = 1990.79$	$P(t) = 3.3021 \pm 0.0022$	$\langle \phi_{\min,1} \rangle_{\mathrm{obs}} = 5.81 \pm 0.14$	
$\phi_{\min,1}$=5.66(SET=57)	$\phi_{\min,1}$=5.96(SET=58)	$\phi_{\min,1}$=5.71(SET=59)	$\phi_{\min,1}$=5.96(SET=60)	$\phi_{\min,1}$=5.79(SET=61)
$\phi_{\min,1}$=5.79(SET=62)	$\phi_{\min,1}$=6.00(SET=63)	$\phi_{\min,1}$=5.93(SET=64)	$\phi_{\min,1}$=5.62(SET=65)	$\phi_{\min,1}$=5.71(SET=66)
PHOT1991 prediction:	$\Delta t = 276.4$	$P_{\mathrm{pred}} = 3.2876 \pm 0.0015$	$\langle \phi_{\min,1} \rangle_{\mathrm{pred}} = 5.98 \pm 0.15$	$\mathrm{RES} = 0.38$
PHOT1991	$\langle t \rangle = 1991.55$	$P(t) = 3.2731 \pm 0.0020$	$\langle \phi_{\min,1} \rangle_{\mathrm{obs}} = 6.36 \pm 0.16$	
$\phi_{\min,1}$=6.33(SET=67)	$\phi_{\min,1}$=6.37(SET=68)	$\phi_{\min,1}$=6.43(SET=69)	$\phi_{\min,1}$=6.26(SET=70)	$\phi_{\min,1}$=6.17(SET=72)
$\phi_{\min,1}$=6.24(SET=71)	$\phi_{\min,1}$=6.37(SET=73)	$\phi_{\min,1}$=6.38(SET=74)	$\phi_{\min,1}$=6.34(SET=75)	$\phi_{\min,1}$=6.23(SET=76)
$\phi_{\min,1}$=6.40(SET=78)	$\phi_{\min,1}$=6.79(SET=79)			
PHOT1992 prediction:	$\Delta t = 395.5$	$P_{\mathrm{pred}} = 3.2775 \pm 0.0010$	$\langle \phi_{\min,1} \rangle_{\mathrm{pred}} = 6.23 \pm 0.16$	$\mathrm{RES} = 0.26$
PHOT1992	$\langle t \rangle = 1992.63$	$P(t) = 3.28189 \pm 0.00056$	$\langle \phi_{\min,1} \rangle_{\mathrm{obs}} = 5.97 \pm 0.04$	
$\phi_{\min,1}$=5.89(SET=80)	$\phi_{\min,1}$=5.95(SET=82)	$\phi_{\min,1}$=5.96(SET=83)	$\phi_{\min,1}$=6.01(SET=85)	$\phi_{\min,1}$=5.98(SET=87)
$\phi_{\min,1}$=6.01(SET=88)	$\phi_{\min,1}$=5.97(SET=89)	$\phi_{\min,1}$=5.95(SET=90)		
PHOT1993 prediction:	$\Delta t = 363.5$	$P_{\mathrm{pred}} = 3.28797 \pm 0.00041$	$\langle \phi_{\min,1} \rangle_{\mathrm{pred}} = 6.20 \pm 0.05$	$\mathrm{RES} = 0.17$
PHOT1993	$\langle t \rangle = 1993.63$	$P(t) = 3.29405 \pm 0.00061$	$\langle \phi_{\min,1} \rangle_{\mathrm{obs}} = 6.03 \pm 0.17$	
$\phi_{\min,1}$=5.91(SET=92)	$\phi_{\min,1}$=5.89(SET=93)	$\phi_{\min,1}$=5.95(SET=94)	$\phi_{\min,1}$=5.95(SET=97)	$\phi_{\min,1}$=5.98(SET=99)
$\phi_{\min,1}$=5.96(SET=100)	$\phi_{\min,1}$=6.04(SET=103)	$\phi_{\min,1}$=6.20(SET=104)	$\phi_{\min,1}$=6.42(SET=105)	
PHOT1994 prediction:	$\Delta t = 331.4$	$P_{\mathrm{pred}} = 3.3165 \pm 0.0012$	$\langle \phi_{\min,1} \rangle_{\mathrm{pred}} = 7.11 \pm 0.18$	$\mathrm{RES} = 0.36$
PHOT1994	$\langle t \rangle = 1994.53$	$P(t) = 3.3389 \pm 0.0023$	$\langle \phi_{\min,1} \rangle_{\mathrm{obs}} = 7.47 \pm 0.24$	
$\phi_{\min,1}$=7.29(SET=106)	$\phi_{\min,1}$=7.35(SET=107)	$\phi_{\min,1}$=7.38(SET=108)	$\phi_{\min,1}$=7.44(SET=109)	$\phi_{\min,1}$=7.89(SET=110)
PHOT1995 prediction:	$\Delta t = 429.0$	$P_{\mathrm{pred}} = 3.3250 \pm 0.0012$	$\langle \phi_{\min,1} \rangle_{\mathrm{pred}} = 9.20 \pm 0.25$	$\mathrm{RES} = 0.06$
PHOT1995	$\langle t \rangle = 1995.71$	$P(t) = 3.31117 \pm 0.00084$	$\langle \phi_{\min,1} \rangle_{\mathrm{obs}} = 9.26 \pm 0.23$	
$\phi_{\min,1}$=8.97(SET=111)	$\phi_{\min,1}$=9.16(SET=112)	$\phi_{\min,1}$=9.43(SET=113)	$\phi_{\min,1}$=9.46(SET=114)	

shifts from solar equator (smallest P) to the highest latitudes (largest P).

Finally, the predictiveness of the yearly ephemerides was tested by checking whether the $\phi_{\min,1}$ changes in V 1794 Cyg qualitatively resemble the continuous O–C modulations of eclipsing binaries (e.g. Jetsu et al. 1997). Such continuity would indicate that the activity centres survive the disruptive influence of differential rotation and/or latitudinal migration. But the yearly predictions failed (Table 4). Nevertheless, *only one abrupt $\phi_{\min,1}$ shift was observed on September 1990*, while the other $\phi_{\min,1}$ discontinuities coinciding with observational gaps could not be reliably established (Fig. 9).

We encountered several manifestations of the solar–stellar–connection in the long–term photometry of V 1794 Cyg, and our time series analysis leaves an impression that unpredictability is one of the foremost characteristics for magnetic activity in this object.

Acknowledgements. The work was partly supported by the EC Human Capital and Mobility (Networks) project "Late type stars: activity, magnetism, turbulence" No. ERBCHRXCT940483. This research has made use of the Simbad–database operated at CDS, Strasbourg, France.

References

Berdyugina S.V., Tuominen I., 1998, A&A 336, L25
Bopp B.W., Rucinski S.M., 1981, In: Sugimoto D., Lamb D.Q., Schramm D.N. (eds.) Fundamental Problems in the Theory of Stellar Evolution. I.A.U. Symp. 93, p. 177
Bopp B.W., Stencel R.E., 1981, ApJ 247, L131
Böhm–Vitense E., 1992, AJ 103, 608
Carrington R.C., 1858, MNRAS 19, 1
Dempsey R.C., Bopp B.W., Henry G.W., Hall D.S., 1993, ApJS 86, 293
Drake S.A., Walter F.M., Florkowski D.R., 1990, In: Wallerstein G. (ed.) Sixth Cambridge Workshop on Cool Stars, Stellar Systems, and the Sun. PASPC 9, p. 148
Eaton J.A., Hall D.S., 1979, ApJ 227, 907
Fekel F.C., 1997, PASP 109, 514
Hall D.S., 1972, PASP 84, 323
Hall D.S., 1987, Publ. Astr. Inst. Czechoslovakia 70, 77
Hall D.S., 1991, In: Tuominen I., Moss D., Rüdiger G. (eds.) The Sun and Cool Stars: activity, magnetism, dynamos. I.A.U. Coll. 130, Springer–Verlag, Heidelberg, p. 353
Hall D.S., Busby M.R., 1990, In: Ibanoğlu C. (ed.) Active Close Binaries. Kluwer, Dordrecht, p. 377
Hartmann L.W., Noyes R.W., 1987, ARA&A 25, 271
Henry G.W., Newsom M.S., 1996, PASP 108, 242
Henry G.W., Eaton J.A., Hamer J., Hall D.S., 1995, ApJS 97, 513
Herbig G.H., 1958, ApJ 128, 259
Howard R.F., 1994, In: Balasubramaniam K.S., Simon G.W. (eds.) Solar Active Region Evolution: Comparing Models with Observations. PASPC 68, p. 1
Huenemoerder D.P., 1986, AJ 92, 673
Jetsu L., 1996, A&A 314, 153
Jetsu L., Pelt J., 1996, A&AS 118, 587 (Paper III)
Jetsu L., Pelt J., 1999, A&AS, in press (Paper I)
Jetsu L., Huovelin J., Tuominen I., et al., 1990a, A&A 236, 423
Jetsu L., Huovelin J., Tuominen I., et al., 1990b, A&AS 85, 813
Jetsu L., Pelt J., Tuominen I., 1993, A&A 278, 449
Jetsu L., Pagano I., Moss D., et al., 1997, A&A 326, 698
Jetsu L., Tuominen I., Bopp B.W., et al., 1999, A&AS, in press (Paper II)
Kron G.E., 1947, PASP 59, 261
Kuiper N.H., 1960, Proc. Koningkl. Nederl. Akad. Van Wettenschappen, Series A 63, 38
Maunder E.W., 1890, MNRAS 50, 251
Maunder E.W., 1894, Knowledge 17, 173
Pasquini L., Brocato E., Pallavicini R., 1990, A&A 234, 277
Schachter J.F., Remillard R., Saar S.H., et al., 1996, ApJ 463, 747
Schwabe H., 1843, Astr. Nachr. 21, 233
Simon T., Fekel F.C., 1987, ApJ 316, 434
Strassmeier K.G., Fekel F.C., Bopp B.W., Dempsey R.C., Henry G.W., 1990, A&AS 72, 191
Swanepoel J.W.H., De Beer C.F., 1990, ApJ 350, 754
Walter H.G., Hering R., de Vegt Ch., 1990, A&AS 86, 357
Willson R.C., Hudson H.S., 1991, Nat 351, 42
Zeilik M., 1991, In: Tuominen I., Moss D., Rüdiger G. (eds.) The Sun and Cool Stars: activity, magnetism, dynamos. I.A.U. Coll. 130, Springer–Verlag, Heidelberg, p. 370